ISSN 1063-7834, Physics of the Solid State, 2009, Vol. 51, No. 10, pp. 2077–2083. © Pleiades Publishing, Ltd., 2009.
Original Russian Text © G.A. Petrakovskiĭ, L.N. Bezmaternykh, D.A. Velikanov, A.M. Vorotynov, O.A. Bayukov, M. Schneider, 2009, published in Fizika Tverdogo Tela, 2009, Vol. 51, No. 10, pp. 1958–1964.

MAGNETISM
AND FERROELECTRICITY

Magnetic Properties of Single Crystals of Ludwigites Cu_2MBO_5 ($M = Fe^{3+}$, Ga^{3+})

G. A. Petrakovskiĭ[a, b], L. N. Bezmaternykh[a], D. A. Velikanov[a], A. M. Vorotynov[a, *], O. A. Bayukov[a, b], and M. Schneider[c]

[a] *Kirensky Institute of Physics, Siberian Branch, Russian Academy of Sciences, Akademgorodok, Krasnoyarsk, 660036 Russia*
* *e-mail: sasa@iph.krasn.ru*
[b] *Siberian Federal University, pr. Svobody 79, Krasnoyarsk, 660041 Russia*
[c] *Paul Scherrer Institut, Villigen, 5232 Switzerland*

Received November 11, 2008; in final form, February 10, 2009

Abstract—High-quality single crystals of ludwigites Cu_2MBO_5 ($M = Fe^{3+}$, Ga^{3+}) have been grown, and the magnetic, resonance, and Mössbauer studies have been performed. It is established that the Cu_2FeBO_5 and Cu_2GaBO_5 compounds are antiferromagnets with Néel temperatures of 32 and 3.4 K, respectively. A model of the magnetic structure of the compounds is proposed. It is shown that the magnetic properties of the ludwigites are substantially dependent on the degree of ion distribution over crystallographic positions.

PACS numbers: 75.10.-b, 75.25.+z, 75.30.-m

DOI: 10.1134/S106378340910014X

1. INTRODUCTION

Boroferrites with a $Me^{2+}M^{3+}BO_5$ ludwigite structure are orthorhombic crystals with space group *Pbam* [1]. By now, we know a wide set of both natural and synthetic ludwigites in which cations are Me^{2+} = Mg, Ni, Co, Fe, and Cu; and M^{3+} = Fe, Mn, Co, Ti, and Al [1–5].

According to [5–14], these materials are low-dimensional magnets. It is assumed that the magnetic structure of these crystals can be represented as two-dimensional layers and the distribution of magnetically active cations provides the separation of the structure into two weakly coupled magnetic subsystems. One of the subsystems is mainly occupied with the Me^{2+} cations, and the other subsystem is mainly occupied with the M^{3+} cations. This assumption is based on the peculiarities experimentally observed in the temperature dependences of the magnetic susceptibility and differential thermal analysis.

The copper ludvigites studied in this work are variants of the *Pbam* structure distorted because of the Jahn–Teller effect and have space group $P2_1/c$ [15]. The crystal lattice parameters are $a = 3.108$ Å, $b = 12.003$ Å, $c = 9.459$ Å, $\beta = 96.66°$, and $z = 4$ for Cu_2FeBO_5 and $a = 3.1146$ Å, $b = 11.921$ Å, $c = 9.477$ Å, $\beta = 97.91°$, and $z = 4$ for Cu_2GaBO_5. The magnetic properties of Cu_2FeBO_5 were measured in [16]; it was revealed that the Cu and Fe subsystems are ordered independently of one another. In our opinion, it is important to study the magnetic properties of Cu_2FeBO_5 and Cu_2GaBO_5 on high-quality single crystals. In particular, this will allow one to separate contributions of Cu^{2+} ($S = 1/2$) and Fe^{3+} ($S = 5/2$) ions to the formation of the magnetic state of the compounds.

In this work, we study the temperature dependences of the magnetic susceptibility of Cu_2FeBO_5 and Cu_2GaBO_5 single crystals, the field dependences of the magnetization at a temperature of 1.8 K, and the Mössbauer spectra of Cu_2FeBO_5 at room temperature. The studies show that these ludwigites are antiferromagnets with an incomplete three-dimensional structure of the exchange interactions.

2. SAMPLE PREPARATION

Single crystals of the copper ferroborate Cu_2FeBO_5 were grown from a 51.5 wt % (B_2O_3 + 0.283LiO_2) + 48.5 wt % (CuO + Fe_2O_3) solution–melt, in which Cu_2FeBO_5 is a high-temperature phase with the crystallization range no lower than 80–100°C. Its saturation temperature was T_{sat} = 905–910°C, the slope of the concentration dependence of the saturation temperature was $dT_{sat}/dn = 2$°C/wt %, and the metastable zone width was ΔT_{met} = 10–12°C. The solution–melt 100 g in weight was prepared in a 100-ml platinum crucible by sequential melting of the following reagents at $T = 1000$°C: B_2O_3, 52.1 g; Li_2CO_3, 13.8 g (Li_2O, 5.6 g); CuO, 28.2 g; and Fe_2O_3, 14.1 g.

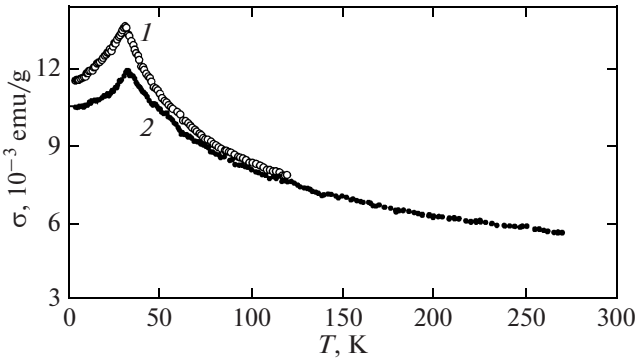

Fig. 1. Temperature dependences of the magnetization of Cu_2FeBO_5 measured in fields of 200 Oe oriented (*1*) perpendicular to the *a* axis and (*2*) along the *a* axis.

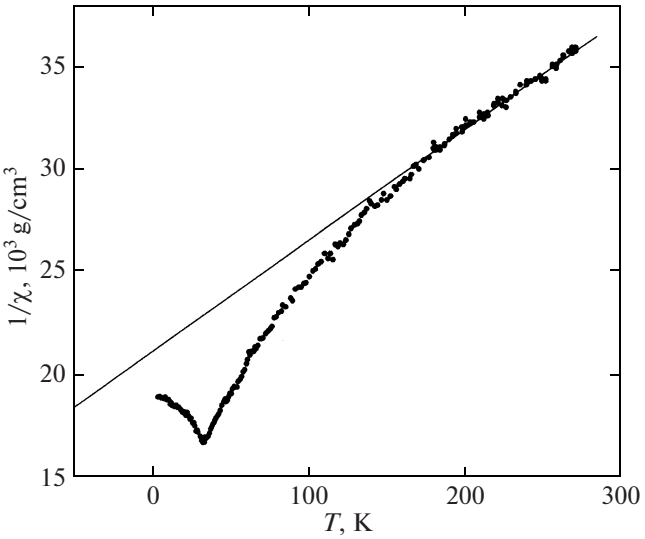

Fig. 2. Temperature dependence of the inverse magnetic susceptibility of Cu_2FeBO_5. The magnetic field is parallel to the *a* axis of the crystal.

The crucible was placed in a crystallization furnace with a nonuniform temperature field so that, at a temperature of 800–900°C, the vertical component of the temperature gradient in the solution–melt was $dT_{sat}/dn = -(1–2)$°C/cm. Sign minus means that the temperature decreases with distance from the crucible bottom. The solution–melt was held at a temperature of 980°C for 24 h to complete dissolution and homogenization. Thereafter, a crystal holder was introduced into the prepared region of the solution–melt, and the solution–melt was cooled at a rate of 100°C/h to a temperature that was 1–3°C lower than the metastability boundary. The spontaneously nucleated crystals were grown then at a smoothly decreasing temperature at a rate $dT_{sat}/dt = 1–3$°C. For three days, the Cu_2FeBO_5 crystals $2 \times 2 \times 15$ mm in size in the form of oblique prisms were grown on the crystal holder. The prisms were extended along the least parameter of the unit cell.

The Cu_2GaBO_5 single crystals were grown following the same technology with the corresponding components of the charge.

3. MAGNETIC MEASUREMENTS

The magnetic properties were measured using a SQUID magnetometer and a PPMS commercial setup. Figure 1 shows the temperature dependences of the magnetization of the Cu_2FeBO_5 single crystal measured in a field of 200 Oe in the temperature range 4.2–270 K for two orientations of the sample. At temperatures $T > 120$ K, the magnetic susceptibility is isotropic, and its temperature dependence follows the Curie–Weiss law. The asymptotic Néel temperature is $\theta_N = -384$ K, which is indicative of a predominantly antiferromagnetic character of the exchange interactions in the spin system (Fig. 2). The Curie–Weiss constant is $C_{exp}^{-1} \approx 56$, while the value calculated from the relationship

$$C_{calc}^{-1} = \{N_0\mu_B^2[2g_{Cu}^2 S_{Cu}(S_{Cu}+1) + g_{Fe}^2 S_{Fe}(S_{Fe}+1)]/3k_B M_{mol}\}^{-1}$$

for $g_{Cu} = g_{Fe} = 2$, $S_{Cu} = 1/2$ and $S_{Fe} = 5/2$ is 53. The proximity of these values testifies that the magnetism of the crystal is really determined by the Cu^{2+} and Fe^{3+} cations. At $T_N = 32$ K, the susceptibility has a maximum, which we identify as the transition of the crystal to the antiferromagnetic state. The dependences presented in Figs. 1 and 2 do not contain additional peculiarities. Our results differ from the results obtained in [16]. The difference is likely related to the use in [6] of a set of small single crystals with a concentration inhomogeneity, whereas we used the high-quality single crystal.

Figure 3 depicts the temperature dependences of the magnetization of the Cu_2GaBO_5 single crystal in the temperature range 1.8–180 K for two orientations of a magnetic field of 50 Oe. The susceptibility anomaly at $T_N = 3.4$ K corresponds to the transition of the spin system to the antiferromagnetic state. In the temperature range 50–180 K, the magnetic susceptibility follows the Curie–Weiss law with the asymptotic Néel temperature θ_N about −60 K (Fig. 4). Thus, the predominant exchange interactions in the magnetic system of the Cu^{2+} ions are antiferromagnetic. The field dependence of the magnetization at the temperature $T = 1.8$ K is shown in Fig. 5. The magnetic saturation is not observed in fields up to 60 Oe.

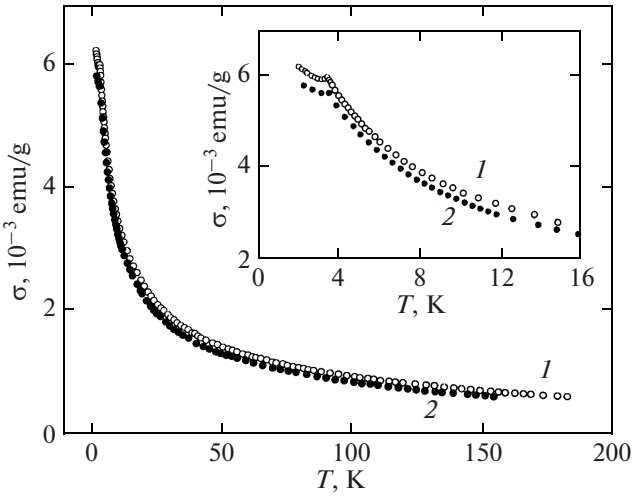

Fig. 3. Temperature dependences of the magnetization of Cu_2GaBO_5 measured in fields of 50 Oe oriented (*1*) along the *a* axis and (*2*) perpendicular to the *a* axis.

4. ELECTRON PARAMAGNETIC RESONANCE MEASUREMENTS

The electron paramagnetic resonance of the crystals was measured on a 3-cm EPR spectrometer in the paramagnetic temperature range 77–300 K. As the Cu_2GaBO_5 crystal is oriented normally to the *a* axis, we observe the resonance with a *g* factor of about 2.173 and an absorption line width ΔH_{pp} of the order of 360 Oe at room temperature. As the temperature decreases to 77 K, the line width and the *g* factor monotonically decrease to 320 Oe and 2.152, respectively.

In the case of the Cu_2FeBO_5 crystal, at the same orientation of the magnetic field, a very broad magnetic resonance line with a Gaussian shape with the parameters $\Delta H_{pp} = 3186$ Oe and $g = 1.81$, which are almost independent of the temperature up to 77 K, is observed.

5. MÖSSBAUER MEASUREMENTS

The Mössbauer measurements were performed with a Co^{57}(Cr) source exhibiting the line width at half-height equal to 0.24 mm/s and an absorber from a sodium nitroprusside powder. Figure 6 shows the spectrum measured at room temperature.

The spectrum interpretation was carried out at two stages. At the first stage, the probability distribution of quadrupole splittings *P*(QS) was determined (see Fig. 7). The peculiarities in this distribution testify that there are possible nonequivalent positions (states) of the iron. The probability distribution gives only qualitative information, since, when fitting, we used one value of the isomer shift common to a group of the doublets. This information was used to construct a model spectrum.

At the second stage, the model spectrum was fitted to the experimental spectrum by varying the overall set of hyperfine structure parameters with the use of the least-squares method in the linear approximation. In the course of the fitting, the parameters of individual doublets were refined. The occupancies of false positions, which are presented in the probability distribution function, become negligibly small. The results of the two-stage identification of the spectrum are given in Table 1.

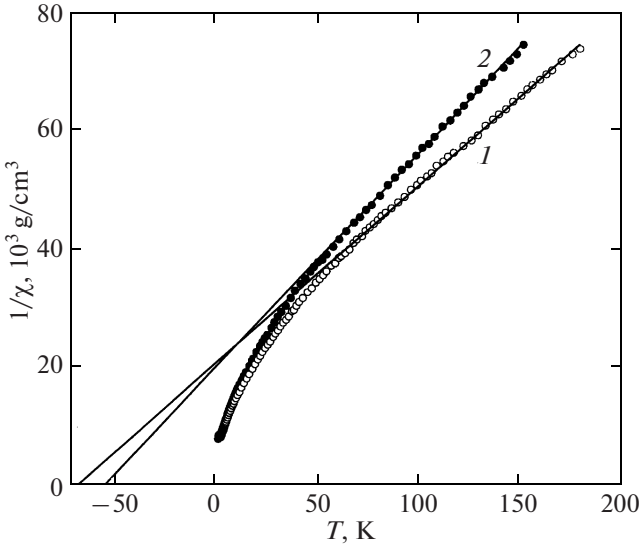

Fig. 4. Temperature dependences of the inverse magnetic susceptibility of Cu_2GaBO_5. The designations are the same as in Fig. 3.

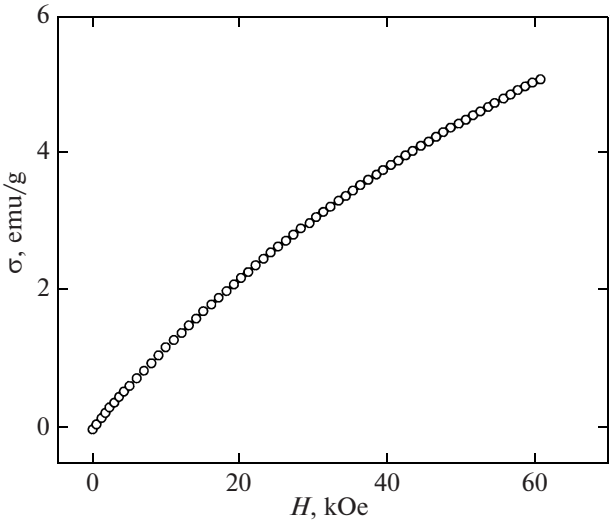

Fig. 5. Field dependence of the magnetization of Cu_2GaBO_5 at $T = 1.8$ K.

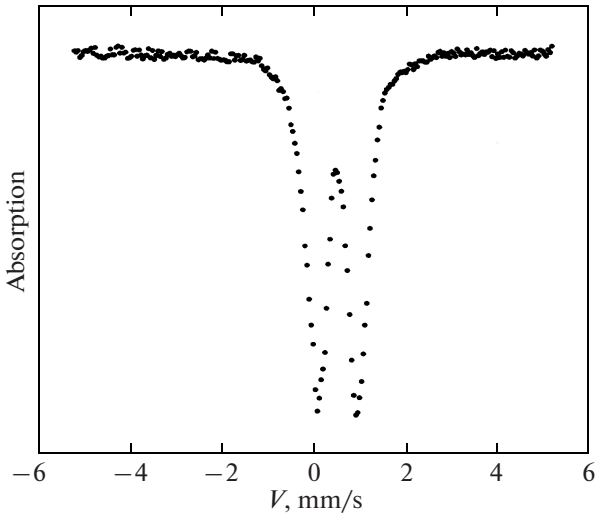

Fig. 6. Mössbauer spectrum of Cu_2FeBO_5 measured at room temperature.

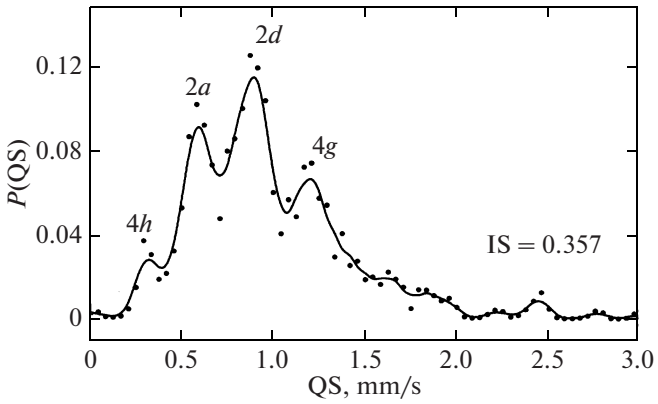

Fig. 7. Probability distribution function of the quadrupole splitting for Cu_2FeBO_5.

The numbering of the crystallographic sublattices is assigned according to the numbering of cations in [15]. The crystallographic positions are denoted as for orthorhombic ludwigites. As was shown in [15], all oxygen octahedra in the ludwigite Cu_2FeBO_5 are distorted. The assignment of a Mössbauer position to a crystallographic position was performed by the degree of distortion of the oxygen octahedron. As the degree of distortion, we take the electric-field gradient V_{zz} induced at the iron site by the nearest coordination octahedron of oxygen ions; that is,

$$V_{zz} \sim \sum 2e\frac{(3\cos^2\theta - 1)}{r^3},$$

where e is the elementary charge, θ is the angle between the principal axis of the electric-field gradient tensor and the direction to the neighboring oxygen anion, and r is the iron–oxygen distance. In principle, to correctly determine the electric-field gradient, we should study the convergence of lattice sums. Such studies performed for the spinel structure show that the lattice sum, to a fairly good accuracy, converges to the contribution of the first coordination shell, which can be logically explained. In insulators, the valence contribution to the electric-field gradient is small. On the other hand, the oxygen anions with a large ionic radius quite well screen the contribution of the far coordination shells. Moreover, making an error in the magnitude, we hope that the estimate of the ratio between values of the electric-field gradient is adequate. The calculated values of V_{zz} are given in Table 1. The measured values of QS are in direct proportion to V_{zz}, which allows us to identify the observed positions.

The Mössbauer measurements show that iron enters, in varying degrees, into all four crystallographic sublattices of the ludwigite. The occupancies are listed in column A of Table 1. For comparison, Table 1 contains the estimates obtained by the X-ray diffraction method. Knowing that the cation distribution is dependent on the crystal synthesis conditions and that the accuracy of the Mössbauer method is higher than that of the X-ray diffraction method, we perform further calculations using the data on the Mössbauer effect. Thus, the ludwigite under study has the following formula:

$$(Cu_{0.26}Fe_{0.24})^{2a}(Cu_{0.01}Fe_{0.49})^{2d}(Cu_{0.75}Fe_{0.25})^{4g} \cdot (Cu_{0.99}Fe_{0.01})^{4h}BO_5.$$

According to the fact that the crystal composition contains two kinds of magnetically active cations, this

Table 1. Parameters of the hyperfine structure of the Mössbauer spectrum of Cu_2FeBO_5: IS is the isomer chemical shift with respect to αFe (±0.01 mm/s), QS is the quadrupole splitting (±0.02 mm/s), W is the absorption line width at half-height (±0.02 mm/s), A is the occupancies of the position with iron (±0.02), and V_{zz} is the electric-field gradient at the iron ion

IS	QS	W	A	Position–sublattice	V_{zz}, e/Å^3	Occupancy according to [15]
0.35	0.36	0.24	0.02	4*h*–4	0.17	0
0.37	0.61	0.24	0.19	2*a*–3	0.30	0
0.36	0.88	0.32	0.39	2*d*–2	0.41	0.33
0.35	1.22	0.47	0.40	4*g*–1	0.53	0.66

ludwigite should be assigned to the system with eight magnetic sublattices. An analysis of the crystal structure shows that, from the standpoint of the indirect exchange coupling, there are three types of exchange interactions with the 90°, 120°, and 180° exchanges in this structure. To estimate the magnitudes of the exchange interactions and magnetic structure, we use a simple model of indirect coupling [17]. Here, we take into account only short metal–oxygen–metal (*Me*–O–*Me*) bonds. The long bonds with the next neighbors of the *Me*–O–*Me*–O–*Me* type are neglected. When determining the occupancies of the e_g orbitals of the Cu^{2+} cation, we include the stretching of the oxygen octahedron. An analysis in the framework of this model allows the conclusion that the ludwigite Cu_2FeBO_5 structure should be described by independent integrals of the indirect exchange cation–cation interaction as follows:

$$J^{90}(\mathrm{FeFe}) = -4c(8b + 3c)U_{\mathrm{Fe}}/75 \approx -4.7\ \mathrm{K},$$

$$J^{90}(\mathrm{FeCu}_x) = -2c[b(U_{\mathrm{Fe}} + U_{\mathrm{Cu}}) - (5b/3 + c)J_{\mathrm{Cu}}]/5 \approx 2.44\ \mathrm{K},$$

$$J^{90}(\mathrm{FeCu}_z) = -c[b(U_{\mathrm{Fe}} + U_{\mathrm{Cu}}) - (13b/3 + 2c)J_{\mathrm{Cu}}]/5 \approx 1.13\ \mathrm{K},$$

$$J^{90}(\mathrm{Cu}_x\mathrm{Cu}_x) = 4bcJ_{\mathrm{Cu}} \approx 14.85\ \mathrm{K},$$

$$J^{90}(\mathrm{Cu}_z\mathrm{Cu}_z) = 2bcJ_{\mathrm{Cu}} \approx 7.43\ \mathrm{K},$$

$$J^{180}(\mathrm{FeFe}) = -4(8b^2/9 + c^2)U_{\mathrm{Fe}} \approx -3.38\ \mathrm{K},$$

$$J^{180}(\mathrm{FeCu}_x) = -2[2b^2(U_{\mathrm{Fe}} + U_{\mathrm{Cu}} - J_{\mathrm{Cu}}/3)/3 - c^2J_{\mathrm{Cu}}]/5 \approx -6.15\ \mathrm{K},$$

$$J^{180}(\mathrm{Cu}_x\mathrm{Cu}_x) = -2b^2(3U_{\mathrm{Cu}} - J_{\mathrm{Cu}})/3 \approx -14.5\ \mathrm{K},$$

$$J^{120}(\mathrm{FeFe}) = J^{180}(\mathrm{FeFe})\cos 60^\circ \approx -1.69\ \mathrm{K},$$

$$J^{120}(\mathrm{FeCu}_x) = J^{180}(\mathrm{FeCu}_x)\cos 60^\circ \approx -3.1\ \mathrm{K},$$

$$J^{120}(\mathrm{FeCu}_z) = 2(8b^2/9 + c^2)J_{\mathrm{Cu}}/5 \approx 1.7\ \mathrm{K},$$

$$J^{120}(\mathrm{Cu}_x\mathrm{Cu}_x) = -2b^2(U_{\mathrm{Cu}} - J_{\mathrm{Cu}}) \approx -7.3\ \mathrm{K},$$

$$J^{120}(\mathrm{Cu}_x\mathrm{Cu}_z) = 4b^2J_{\mathrm{Cu}}/3 \approx 4.9\ \mathrm{K}.$$

Here, the symbols x and z at the Cu_x and Cu_z cations imply that the cation interaction is directed along the short (x) or along the long (z) axis of the oxygen octahedron. The parameters of the ligand–cation electron transfer through the σ bond (b) and π bond (c) are the squares of the coefficients of the electron transfer in the expression for the ligand–cation antibonding molecular orbital. For oxide compounds with a ligand–cation interionic distance of ~2 Å, these

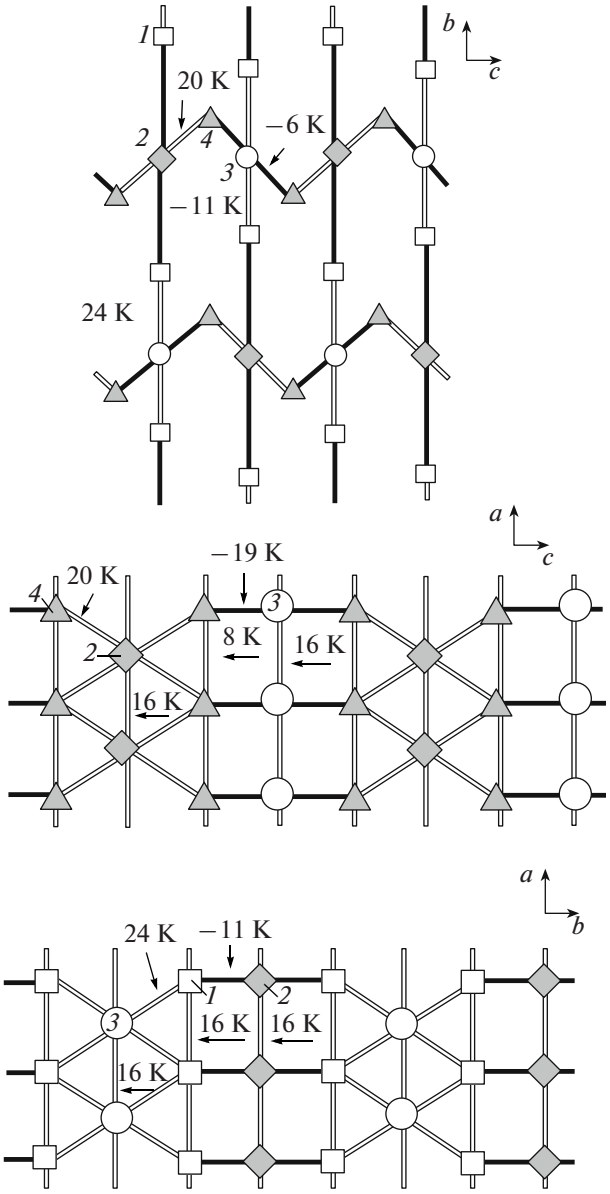

Fig. 8. Schematic representation of the indirect cation–cation interactions in the Cu_2FeBO_5 lattice in the *bc*, *ac*, and *ab* planes.

parameters are $b = 0.02$ and $c \approx 0.01$; $J_{\mathrm{Cu}} \approx 1.6$ eV is the intra-atomic exchange integral for Cu^{2+}. The energies of the ligand–cation electronic excitation for oxide compounds with a hexagonal close packing of oxygen ions are $U_{\mathrm{Fe}} \approx 4$ eV and $U_{\mathrm{Cu}} \approx 2.1$ eV [17].

In principle, knowing the cation–cation exchange interactions, we can estimate the magnetic structure induced by the crystal lattice and the temperature of magnetic ordering. In the case of the eight-sublattice system, the deduction of the formulas for the Néel and Curie temperatures is very complex. We used such an expression for the four-sublattice system [18] by reducing the number of the magnetic sublattices to the

Table 2. Energies of intersublattice exchange interactions in Cu_2FeBO_5 (in K) calculated in terms of the indirect-coupling model

Sublattice	1↑	2↓	3↑	4↓
1↑	16	−11	24.3	15
2↓	−23	16.4	0	39.4
3↑	48.6	0	15.9	−12.2
4↓	15	19.7	−6.2	7.9

Table 3. Energies of intersublattice exchange interactions in Cu_2GaBO_5 (in K) calculated in terms of the indirect-coupling model

Sublattice	1↑	2↓	3↑	4↓
1↑	3.7	−3.6	1.8	0.9
2↓	−7.3	7.4	0	2.0
3↑	3.6	0	0.2	−0.1
4↓	0.9	1.0	−0.05	0.06

number of the crystallographic sublattices. The number of the magnetic bonds and the values of spins were calculated taking into account the Fe^{3+} and Cu^{2+} cations in the crystallographic sublattices. Table 2 is the matrix of calculated energies of the intersublattice interactions for Cu_2FeBO_5 ($E^e = 2J_{ij}S_iS_j$).

This system of interactions leads to a mutual magnetic structure indicated by arrows at the numbers of the sublattices. It turns out that Cu_2FeBO_5 is an antiferromagnet with the Néel temperature $T_N \approx 34$ K, which is very close to an experimental value of 32 K. The frustrating interaction is the interaction between the first and fourth sublattices. Based on the estimates obtained, we can propose a schematic diagram of the magnetic interactions presented in Fig. 8 in the *bc*, *ac*, and *ab* planes of the ludwigite lattice. In this figure, only the magnetically active cations are shown, and the anions and boron cations are not shown. The light and dark symbols indicate the cations with oppositely directed spins. The light and dark bonds mean the ferromagnetic and antiferromagnetic indirect exchange couplings, respectively. The frustrating *Me*1–*Me*4 bonds are omitted. It is seen from Fig. 8 that the cations of sublattices *1* and *2* form the flat walls in the *ab* plane, and the cations of sublattices *2*, *3*, and *4* form the zigzag walls in the *ac* plane. The two mutually perpendicular walls are jointed into the three-dimensional magnetic structure by means of cations of sublattices *2* and *3*. Thus, cations *2* and *3* are exchange-coupled in three dimensions and cations *1* and *4* are exchange-coupled only in two dimensions. Such a lattice is called a magnetically incomplete three-dimensional lattice. The incompleteness of the magnetic lattice and the presence of the frustrating interactions provide a relatively low temperature of magnetic ordering as compared, for example, to copper ferrite [18].

In the analysis of the exchange interactions in Cu_2GaBO_5, we used the data obtained in [15] on the determination of the distribution of the Cu^{2+} and Ga^{3+} cations over the sublattice sites of this ludwigite. According to these data, Ga^{3+} is arranged only in two crystallographic sublattices 2*d*(3) and 4*h*(4) with occupancies of 0.6 and 0.7, respectively. This ludwigite contains only one sort of magnetic cations, and, because of this, Cu_2GaBO_5 is a four-sublattice magnet. Taking into account the concentration of the magnetically active cations in the sublattices, when estimating the number of the magnetic bonds and effective spin of the sublattices, we obtain the matrix of the energies of the intersublattice interactions given in Table 3. The system of the exchange interactions in Cu_2GaBO_5 is identical to that in Cu_2FeBO_5 and must lead to a similar magnetic structure. The Néel temperature calculated using the magnitude of the interactions estimated for Cu_2GaBO_5, is 12 K, which is significantly higher than the experimental temperature $T_N = 3$ K. In principle, this discrepancy may be attributed to imperfection of the indirect-coupling model and the approximations made.

Another reason of the discrepancy between the experimental and calculated Néel temperatures may be the difference between the Ga^{3+} cation distribution in the 4*g* and 2*a* positions in the crystal under study and the distribution presented in [15]. It is known that this type of compounds is prone to a substantial redistribution of ions over the crystal lattice positions depending on the conditions of their synthesis. The expression for T_N testifies that the appearance of Ga^{3+} in the 4*g* and 2*a* positions sharply decreases the Néel temperature.

The results of our studies are strongly different from the results obtained in [16] for Cu_2FeBO_5. First, we revealed only one peculiarity in the temperature dependence of the magnetic susceptibility at 32 K, whereas three peculiarities were observed in [16] at 20, 38, and 63 K. Second, the asymptotic Néel temperature measured in this work $T_N = -384$ K differs from a temperature of −178 K found in [16]. We assume that the reason of the discrepancy is a possible concentration inhomogeneity of the cation distribution in the crystals used in the magnetic measurements [6].

6. CONCLUSIONS

The magnetic measurements and analysis of the exchange interactions show that ludwigites Cu_2FeBO_5 and Cu_2GaBO_5 are antiferromagnets with Néel temperatures of 32 and 3 K, respectively. An incompleteness of the three-dimensional magnetic structure and the presence of the frustrating interaction provide a

relatively low temperature of magnetic ordering. We assume that the magnetic properties of this type of compounds are substantially dependent on the degree of cation distribution over crystallographic positions.

REFERENCES

1. E. F. Bertaut, Acta Crystallogr. **3**, 473 (1950).
2. Y. Takeuchi, T. Watanabe, and T. Ito, Acta Crystallogr. **3**, 98 (1950).
3. R. Norrestam, K. Nielsen, I. Sotofte, and N. Thorup, Z. Kristallogr. **189**, 33 (1989).
4. J. A. Hriljac, R. D. Brown, A. K. Cheetham, and L. C. Satec, J. Solid State Chem. **84**, 289 (1990).
5. J. C. Fernandes, R. B. Guimaraes, M. Mir, M. A. Continentino, H. A. Borges, A. Sulpice. J.-L. Tholence, J. L. Siqueira, L. I. Zawislak, J. B. M. da Gunha, and C. A. dos Santos, Phys. Rev. B: Condens. Matter **58** (1), 287 (1998).
6. H. Neuendorf and W. Gunβser, J. Magn. Magn. Mater. **173**, 117 (1997).
7. J. C. Fernandes, R. B. Guimaraes, M. Mir, M. A. Continentino, H. A. Borges, G. Cernicchiaro, M. B. Fontes, and E. M. Baggio-Saitovitch, Physica B (Amsterdam) **281–282**, 694 (2000).
8. M. A. Continentino, B. Boechart, R. B. Guimataes, J. C. Fernandes, and L. Chivelder, J. Magn. Magn. Mater. **226–230**, 427 (2001).
9. R. B. Guimaraes, M. Mir, J. C. Fernandes, M. A. Continentino, H. A. Borges, G. Cernicchiaro, M. B. Fontes, D. R. S. Candela, and E. Baggio-Saitovitch, Phys. Rev. B: Condens. Matter **60** (9), 6617 (1999).
10. M. Mir, R. B. Guimaraes, J. C. Fernandes, M. A. Continentino, A. C. Doriguetto, Y. P. Mascarenhas, J. Ellena, E. E. Castellano, R. S. Frietas, and L. Chivelder, Phys. Rev. Lett. **87** (14), 147201-1 (2001).
11. M. Matos, E. V. Anda, J. C. Fernandes, and R. B. Guimaraes, J. Mol. Struct. **539**, 181 (2001).
12. J. A. Larrea, D. R. Sanchez, E. M. Baggio-Saitovitch, J. C. Fernandes, R. B. Guimaraes, M. A. Continentino, and F. J. Litterst, J. Magn. Magn. Mater. **226–230**, 12079 (2001).
13. R. B. Guimaraes, M. Mir, M. A. Continentino, J. C. Fernandes, M. B. Fontes, E. S. Yugue, E. M. Baggio-Saitovitch, A. M. Moreira, and N. L. Speziali, J. Magn. Magn. Mater. **226–230**, 1983 (2001).
14. J. C. Fernandes, R. B. Guimaraes, M. A. Continentino, L. Ghivelder, and R. S. Freitas, Phys. Rev. B: Condens. Matter **61** (2), R850 (2000).
15. J. Schaefer and K. Bluhm, Z. Anorg. Allg. Chem. **621**, 571 (1995).
16. M. A. Continentino, J. C. Fernandes, R. B. Guimaraes, H. A. Borges, A. Sulpice, J.-L. Tholence, J. L. Siqueira, J. B. M. da Gunha, and C. A. dos Santos, Eur. Phys. J. B **9**, 613 (1999).
17. O. Bajukov and A. Savitskii, Phys. Status Solidi B **155** (2), 249 (1989).
18. S. Krupicka, *Physik der Ferrite und der verwandten magnetischen Oxide* (Academia, Prague, 1973; Mir, Moscow, 1976), Vol. 1 [in German and in Russian].

Translated by Yu. Ryzhkov